

Water Resources Research

RESEARCH ARTICLE

10.1029/2022WR032073

Key Points:

- Seasonal variations in evapotranspiration (ET) bias groundwater level recession rates in shallow aquifers
- Seasonal recharge estimates from Water Table Fluctuation method can be markedly different depending on whether seasonal variations in recession rates are accounted or not
- Two novel methods to quantify ET's influence on groundwater recession, and consequently on seasonal recharge, are presented

Supporting Information:

Supporting Information may be found in the online version of this article.

Correspondence to:





M. Kumar,
mkumar4@eng.ua.edu

Citation:

Boumis, G., Kumar, M., Nimmo, J. R., & Clement, T. P. (2022). Influence of shallow groundwater evapotranspiration on recharge estimation using the water table fluctuation method. *Water Resources Research*, 58, e2022WR032073. <https://doi.org/10.1029/2022WR032073>

Received 24 JAN 2022
Accepted 3 OCT 2022

Influence of Shallow Groundwater Evapotranspiration on Recharge Estimation Using the Water Table Fluctuation Method

Georgios Boumis¹ , Mukesh Kumar¹ , John R. Nimmo² , and T. Prabhakar Clement¹ 

¹Department of Civil, Construction, and Environmental Engineering, University of Alabama, Tuscaloosa, AL, USA,

²Unsaturated Flow Research, Menlo Park, CA, USA

Abstract Groundwater recharge moves downward from the land surface and reaches the groundwater to replenish aquifers. Despite its importance, methods to directly measure recharge remain cost and time-intensive. Recharge is usually estimated using indirect methods, such as the widely used water-table fluctuation (WTF) method, which is based on the premise that rises in groundwater levels are due to recharge. In the WTF method, recharge is calculated as the difference between the observed groundwater hydrograph and the hydrograph obtained in the absence of water input. The hydrograph in the absence of rise-producing input is estimated based on a characteristic master recession curve (MRC), which describes an average behavior for a declining water-table. Previous studies derive MRC using recession data from all seasons. We hypothesize that for sites where groundwater table is shallow, using recession data from periods with high groundwater-influenced evapotranspiration (ET) rates versus all periods will yield significantly different MRC, and consequently different estimates of recharge. We test this hypothesis and show that groundwater recession rates are significantly greater in warm months when the groundwater-influenced ET rates are higher. Since obtaining seasonal recession rates is challenging for locations with a limited amount of data and is prohibitive if it is to be obtained for any given season of a particular year, we propose two novel parsimonious methods to obtain recession time constants for distinct seasons. The proposed methods show the potential to significantly improve the estimates of seasonal recession time constants and provide a better understanding of seasonal variations in recharge estimates.

1. Introduction

Groundwater is a vital resource for both natural ecosystems and humans (Wada et al., 2014). Over 2 billion people rely on groundwater as their main freshwater resource (Famiglietti, 2014). Groundwater is also extensively used in irrigated agriculture (Siebert et al., 2010). The increased water extraction to satisfy human needs has led to groundwater depletion in many parts of the world (Aeschbach-Hertig & Gleeson, 2012; Rodell et al., 2009; Scanlon et al., 2007). Given these evolving challenges, which are expected to get worse with increasing population, assessment of groundwater recharge, that is, the amount of water that replenishes aquifers after escaping the vadose zone (Healy & Cook, 2002), is crucial for sustainable management and development of groundwater resources (Moon et al., 2004). Groundwater recharge is, however, an inherently complex process controlled by multiple factors including climate, geomorphology, vegetation characteristics and antecedent soil moisture conditions, among others (De Vries & Simmers, 2002). Several methods to obtain estimates of groundwater recharge exist, including those based on direct measurements (Flint et al., 2002) and indirect methods that often use empirical models (Reitz & Sanford, 2020), physically based land surface models (Li et al., 2021; Niraula et al., 2017) or integrated hydrologic models (Kollet & Maxwell, 2006; Kumar & Duffy, 2015; Kumar et al., 2009; Therrien et al., 2010). A majority of the aforementioned methods, however, either involve multiple sources of uncertainty or provide poor time localization (Delin et al., 2007; Heppner et al., 2007; Moeck et al., 2016; Scanlon et al., 2002).

The water-table fluctuation (WTF) method is one of the most widely used approaches to estimate local groundwater recharge, mainly because it is based on easily available measured water-table level variations (Healy, 2010). In its original form, the WTF method is appropriate for shallow unconfined aquifers that display short-term rises of the water-table level in response to rainfall events (Sophocleous, 1991). However, the initial formulation of WTF neglects the fact that the water-table is in a continuous state of recession due to drainage to the closest

surface water body (e.g., a river or lake). A master recession curve (MRC) technique can be used in conjunction with the WTF to compensate for the unrealized recession process, and thus predict the water-table level when it is declining in the absence of a rise-producing input (Heppner & Nimmo, 2005). Such an MRC approach, which requires deriving a characteristic recession behavior from a sufficient record of water-table heads, has been previously utilized in several studies concerning groundwater recharge estimation. For example, in North Carolina (NC), Tashie et al. (2016) employed an MRC coupled with an event-based modification of WTF (Nimmo et al., 2015), to examine long-term relationships between recharge to precipitation ratios and rainstorm characteristics (magnitude, duration, intensity etc.). In another study, Allocca et al. (2015) followed a similar methodology to estimate groundwater recharge in a perched karst aquifer in southern Italy, and evaluated the correlation between recharge and soil water content. Groundwater recharge computed with an episodic master recession approach was also used to evaluate the effects of stormwater infiltration facilities on groundwater systems in Maryland (Bhaskar et al., 2018).

Based on the fact that the MRC technique is being extensively applied to groundwater recharge estimation, it is critical to assess its possible limitations, and quantify consequent impacts on recharge estimation. A major concern regarding the use of an MRC (see also Hung Vu & Merkel, 2019; Thomas et al., 2016; Young et al., 2020), is that the variational behavior of hydrograph recession is lost, despite the fact that water-table recession greatly varies depending on seasonality, subsurface properties, pre-storm conditions etc (Nimmo & Perkins, 2018). In the past, there have been efforts to preserve such variations in the water-table recession and derive segmented MRCs in aquifers with evident media stratification (Nimmo & Perkins, 2018), where the porous medium of each layer affects the way groundwater recesses. However, little work has been done toward highlighting and incorporating seasonality effects. Although biases in the observed groundwater recession curves due to seasonal losses have long been known and acknowledged (Tallaksen, 1995), they have been rarely considered in groundwater recharge estimation via groundwater recession analysis.

We hypothesize that for shallow unconfined aquifers, where the water-table is well above the extinction depth or in other words where the groundwater directly contributes to evapotranspiration (ET), marked differences in seasonal groundwater-induced ET rates can bias groundwater recession, and consequently recharge estimation. To test our hypothesis, we first obtain seasonal (cold/warm) MRCs from two sites in the NC Coastal Plain situated in an unconfined surficial aquifer, and then statistically assess the differences in recession rates. Subsequently, we examine differences in groundwater recharge estimates when seasonal MRCs are utilized instead of a single MRC. Given that short observational record or limited number of recession events might preclude estimation of MRC for any given season, we also propose two new parsimonious methods viz., a conceptual model and a multiple linear regression (MLR) model, to assess seasonal recession behavior.

2. Study Sites and Datasets

We selected two US Geological Survey (USGS) shallow groundwater sites in the NC Coastal Plain (see Figure 1). These sites are located in an overall flat region that consists primarily of sandy soils with fine grains, underlain by shallow surficial aquifers (Winner & Coble, 1996). Groundwater table at the two sites ranges from 0.1 to 3.2 m below land surface (*bls*). The sites usually experience 100–150 cm of precipitation per year. The two study sites are part of the USGS climatic-effects network and thus fluctuations in their hydrograph are primarily due to natural changes in storage driven by climate, and not by any human-induced activity (Howe et al., 2005). Daily groundwater level data from the National Water Information System (Goodall et al., 2008) were retrieved by using the *dataRetrieval* R package (Hirsch & De Cicco, 2015). For site JO-035 (34°58'12" latitude, 77°30'12" longitude), we considered a time period of 14 years (2000–2013), whereas 9 years (2000–2008) were considered for site BE-080 (36°14'21" latitude, 77°11'13" longitude). Missing groundwater level data during the concerned periods (~1% and 0.5% respectively) were filled with cubic spline interpolation (Daliakopoulos et al., 2005). For the identification of periods with no or negligible rainfall (necessary for MRC derivation), we used the nearest National Oceanic and Atmospheric Administration (NOAA) precipitation stations at Trenton and Lewiston (Figure 1), located ~17 and ~12 km away from JO-035 and BE-080, respectively. Trenton station had a complete record of daily precipitation measurements, while for Lewiston station, we applied linear interpolation to fill ~1% (32 days) of missing precipitation data. JO-035 received on average annual precipitation of 137 cm during 2000–2013, and the water-table ranged from 0.1 to 3.2 m *bls* (Figure 2c). Land surface elevation at the site is 19.95 m above NAVD88 datum. Similarly, BE-080 which stands 22.56 m above NGVD29 datum, experienced an

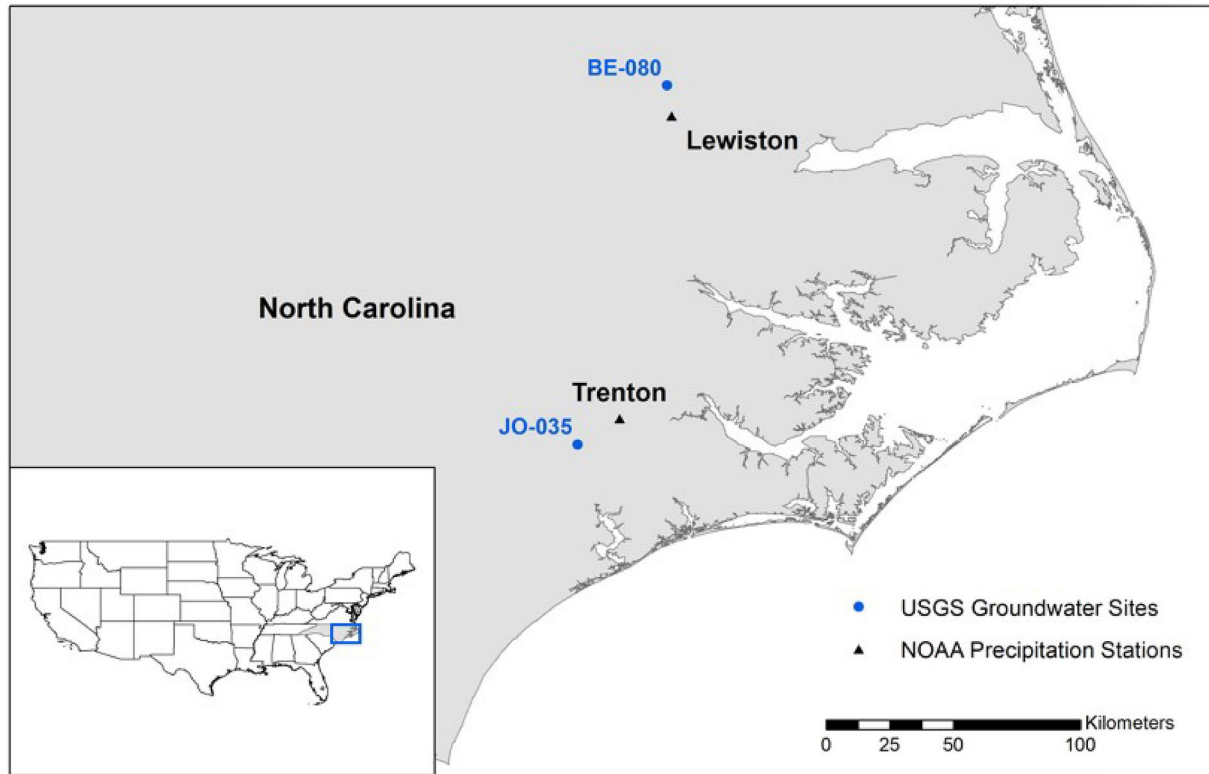


Figure 1. Map of the North Carolina Coastal Plain, with locations of the two groundwater sites used in this study and the locations of nearby meteorological stations.

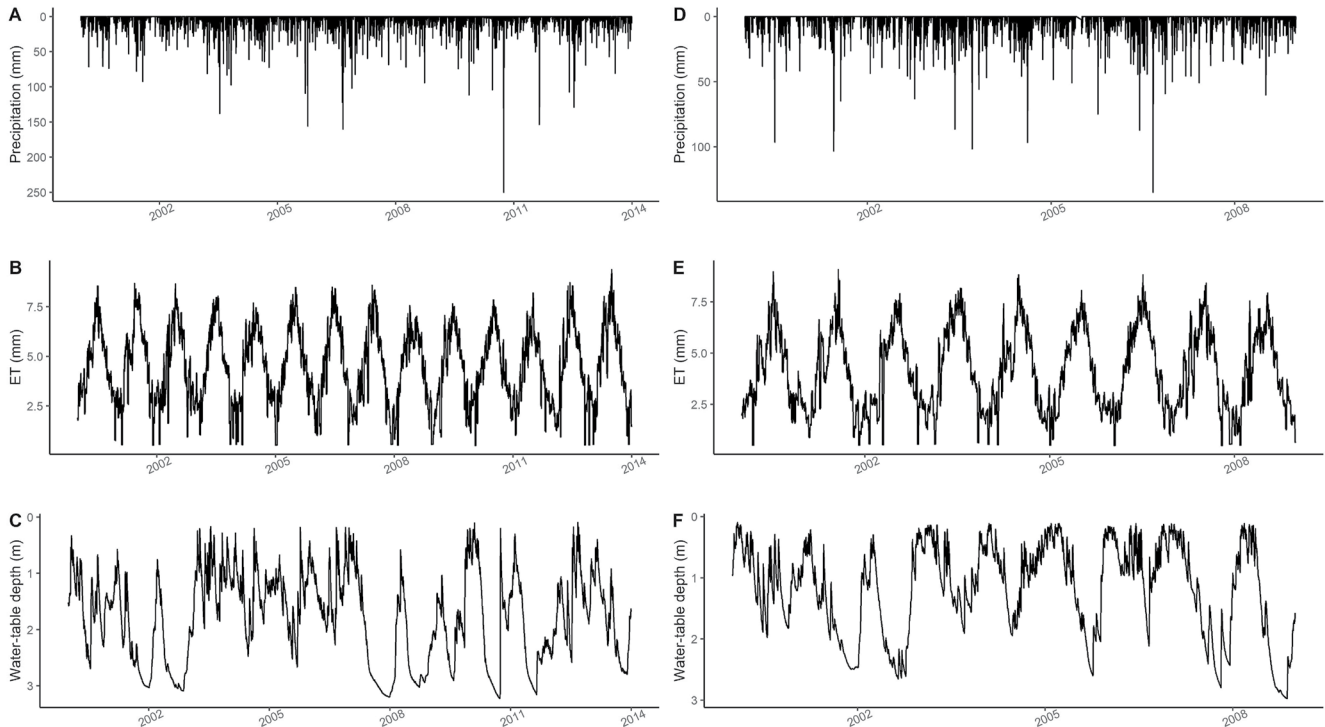


Figure 2. Daily precipitation (a), evapotranspiration (b) and water-table depth (c) at site JO-035 from 1 January 2000 to 31 December 2013. Daily precipitation (d), evapotranspiration (e) and water-table depth (f) at site BE-080 from 1 January 2000 to 31 December 2008.

average annual precipitation of 114 cm, while the water-table ranged from 0.1 to 3.0 m *bfs* (Figure 2f). At both sites, it is likely that the water-table is above the extinction depth and water losses from the aquifer might occur due to ET (Coes et al., 2007; Howe et al., 2005).

In the absence of site-specific ET measurements, which are generally hard to acquire, we relied on ET from remotely sensed data produced by the operational USGS Simplified Surface Energy Balance (SSEBop) model (Senay, 2018; Senay et al., 2013). Daily raster images of 1-km spatial resolution were utilized to obtain the ET time series for both study sites by extracting values from the respective pixel that enclosed each site. Figure 2b displays ET from 2000 to 2013 at site JO-035, indicating a strong seasonal component with summer months exhibiting high ET rates in contrast to winter. The respective time series for site BE-080 shows a similar pattern (see Figure 2e). For the considered time periods, the annual average ET for JO-035 and BE-080 were 162 and 149 cm, respectively. The interrelations of all three variables (precipitation, ET, and water-table depth) at both sites JO-035 and BE-080 are shown for a typical year (2003) in Figures S1 and S2 in Supporting Information S1 respectively. As expected, the water-table at both sites shows high responsiveness to precipitation events. Water-table levels are typically greater in the cold season when the ET losses are lower. Higher ET rates in the warm season cause a decline in the water-table despite the fact that most of precipitation occurs during summer months (Howe et al., 2005).

3. Methods

3.1. Deriving the MRC

In many groundwater systems, it is commonly assumed that the groundwater declines exponentially (Cuthbert, 2014; Rorabaugh, 1960), and so the recession rate is directly proportional to h :

$$\frac{dh}{dt} = -\frac{h}{\tau} \quad (1)$$

where h is water-table elevation [L]; t is time [T] and τ is recession time constant [T], indicative of how fast (slow) the groundwater is recessing. The MRC, is evaluated by first collecting all recession segments from the entire groundwater level time series, and then fitting a linear regression model of the form:

$$\frac{dh}{dt} = b + w * h \quad (2)$$

The τ value is then estimated as the negative reciprocal of the parameter w . Seasonal MRCs can be fitted by following the same procedure as above, using cold season (October to March) and warm season (April to September) data respectively, as opposed to the complete water-table elevation time series. For the identification of hydrograph recessions and the linear fits, we utilized the *MRCfit.v5.1* R program (Nimmo & Perkins, 2018). A representative recession segment is set to at least 7 days of consecutive water-table declines. The program identifies recession segments for which the start of the recession occurs well after significant precipitation has fallen. In that sense, the recession data represent pure recessions that are not significantly affected by residual water traversing the vadose zone down to the water-table. The program, however, also offers the option to tolerate negligible amounts of precipitation during the identified recession period that are not expected to have an effect on the declining water-table. The latter option typically results in the selection of more recession segments.

3.2. The WTF Method

Based on the premise that rises in groundwater levels are due to recharge water arriving at the water-table, groundwater recharge can be computed by (Healy & Cook, 2002):

$$R = \Delta h * s_y \quad (3)$$

where R is recharge [L]; s_y is specific yield [-] and Δh is water-table rise [L]. One way to calculate Δh is by subtracting the minimum water-table elevation from the maximum value during the recharge period, however, this does not account for the ongoing recession process. Once an MRC has been established, a better option is to extrapolate the recessing water-table assuming that no recharge occurs in this period (Heppner & Nimmo, 2005).

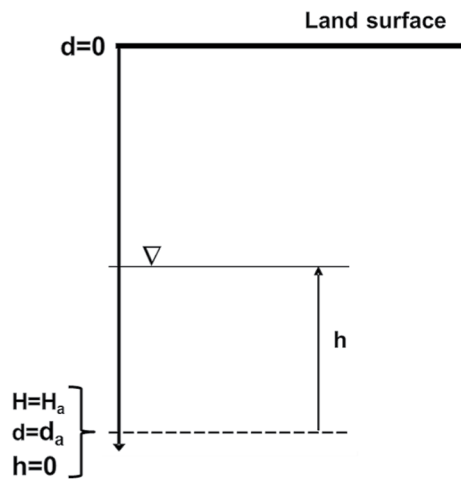


Figure 3. Example of a shallow unconfined aquifer: H_a is root extinction level, d is water-table depth, d_a is the root extinction depth, and h is height of water-table above H_a .

By computing the difference between the groundwater hydrograph and the extrapolated curve for a time interval, an effective Δh (Δh_{eff} , hereafter) can be obtained, and hence recharge for that time interval can be evaluated using:

$$R = \Delta h_{eff} * s_y \quad (4)$$

3.3. A Simple Conceptual Model for Estimating Seasonal Recession Time Constant

To account for the influence of groundwater ET on the seasonality of recession time constant, we first develop a parsimonious conceptual model. Let d denote the water-table depth, d_a is the extinction depth, that is, the depth below which groundwater evapotranspiration is zero (as depicted in Figure 3). If a fraction, $\alpha(t)$, of total ET at the site is from transpiration (q_{ET}), that is, $q_{ET} = \alpha(t)ET$, and assuming that q_{ET} satisfies the following criteria:

1. Both vadose zone water and groundwater are extracted for q_{ET} , over the entire range from $d = 0$ to $d = d_a$. This assumption is reasonable in shallow systems where the root extinction depth d_a is deep enough to extend below the water-table.
2. At all times, roots are equally effective at water extraction, both above and below the water-table. This assumption is reasonable in homogeneous systems where capillary fringe may extend close to land surface.

Then, the portion of q_{ET} coming from the saturated zone, that is, q_{ETS} , can be evaluated as:

$$q_{ETS} = \frac{h * q_{ET}}{d_a} \quad (5)$$

Note that for systems with non-homogenous moisture extraction from the unsaturated and saturated zone, portion of q_{ET} from the saturated zone may be evaluated using a more generic nonlinear (with respect to h) equation such as (Dubois, 1995; Luo et al., 2009):

$$q_{ETS} = \left(\frac{h}{d_a} \right)^{\beta(t)} q_{ET} \quad (6)$$

where $\beta(t)$ may vary in time. However, given the lack of site-specific data of plant root density and depth, subsurface properties, and its heterogeneity, partitioning of ET into evaporation and transpiration, and ancillary hydrologic data to validate the complex soil-root moisture interactions, here we chose to use the simpler, data-parsimonious representation as shown in Equation 5. Specifically, we assumed that $\alpha(t)$ and $\beta(t)$ are equal to 1. The resulting conceptual model is simple enough to study the role of seasonal variations in groundwater ET (q_{ETS}) in modulating recession time constant. The goal here is to assess if this simplistic model, with its inherent assumptions and associated inaccuracies, can still improve seasonal estimates of recession time constants.

In systems where water-table is within the root extinction zone, the observed decline in the water-table results not only from the absence of recharge but also due to the water extracted from the saturated zone by plant roots via ET. As such, we correct Equation 1 using Equation 5 to account for root water extraction:

$$\frac{dh}{dt} = -\frac{h}{\tau} - \frac{q_{ETS}}{s_y} = -h * \left(\frac{1}{\tau} + \frac{q_{ET}}{d_a * s_y} \right) \quad (7)$$

The solution of Equation 7 is the typical exponential decline formula with the recession time constant being equal to the reciprocal of the expression in parenthesis. Hence, the recession time constant of the instantaneous decline of water-table is:

$$\tau_m = \frac{1}{\frac{1}{\tau} + \frac{q_{ET}}{d_a * s_y}} \quad (8)$$

Expression 8 relates the recession time constant, τ_m , which is computed by *MRCfit.v5.1* from the observed hydrograph and has the influence of ET inherent in it, to the recession time constant, τ , that is not affected by ET from groundwater. This expression can be used to relate observed recession time constants for warm (τ_{mW}) and cold (τ_{mC}) seasons by accounting for the influence of ET rates of the respective seasons using the equations:

$$\frac{1}{\tau_{mW}} = \frac{1}{\tau} + \frac{q_{ETW}}{d_a * s_y} \quad (9)$$

$$\frac{1}{\tau_{mC}} = \frac{1}{\tau} + \frac{q_{ETC}}{d_a * s_y} \quad (10)$$

where q_{ETW} and q_{ETC} indicate average ET flux extracted from the groundwater for warm and cold seasons respectively. Equations 9 and 10 can be solved to obtain τ and d_a . Either of the two equations may then also be used to derive recession time constants for a warm or cold season or any alternative season or time period (e.g., Mar-May) by just using τ , d_a , and q_{ET} for the period under consideration. Such evaluation of τ_m could especially be useful for settings with a limited length of groundwater time series or a scant number of recharge events or with only a few no-recharge recession events as identified by *MRCfit.v5.1*, as these may preclude estimation of τ_m directly from the observed groundwater time series. Notably, estimation of seasonal or within-year τ_m for any given year is usually prohibitive because it lacks a sufficient number of identified recession events. Equations 9 and 10 can, however, provide such estimates.

3.4. MLR Model for Estimating Seasonal Recession Time Constant

Given the outlined uncertainties in the formulation of the functional relation (see Subsection 3.3) to assess q_{ETS} or the plant water extraction from the saturated zone, and thus in quantifying the influence of q_{ETS} on recession time constant, we also explore an alternative data-driven formulation. Here we estimate τ_m as a parsimonious linear function of these two variables based on the equation:

$$\tau_m = b + w_1 * H + w_2 * ET \quad (11)$$

where H and ET are average water-table level and evapotranspiration rate. Notably, if derivation of Equation 7 was performed using Equation 6 instead of Equation 5, τ_m in Equation 8 would also be dependent on both ET and H, as is the case here in Equation 11. As the estimation of τ_m (which is inherently influenced by ET) using MRC method generally requires $\frac{dh}{dt}$ and h for multiple recession events, here we generate $(\frac{dh}{dt}, h)$ for k sets of recession events out of n total number of recession segments (identified by *MRCfit.v5.1* from the observed hydrograph). Each set consists of $(n-k)$ recession events - here, we set $(n-k)$ approximately equal to the number of seasonal recessions (see Subsection 4.1) to allow for a robust estimate of τ_m within each set. To identify these k sets, all n recession events were first listed in increasing order of ET. The first set included recession events with index ranging from 1 to $(n-k)$, the second ranged from 2 to $(n-k+1)$ and the k th set ranged from k to n . This design ensured that each set has a median ET rate that is distinct from other sets. Consequently, parameters of the linear regression are derived using the τ_m , median H and median ET rate of each set. Knowing the parameters of Equation 11 then would allow for the estimation of the average recession time constant for any given period (a season, or even a month), provided the average water-table height and ET rate of that period is known. This model provides a data-driven alternative to the conceptual model presented in the previous subsection, and it could also be useful for deriving seasonal recession time constants for settings with a limited number of *MRCfit.v5.1*-identified recession events.

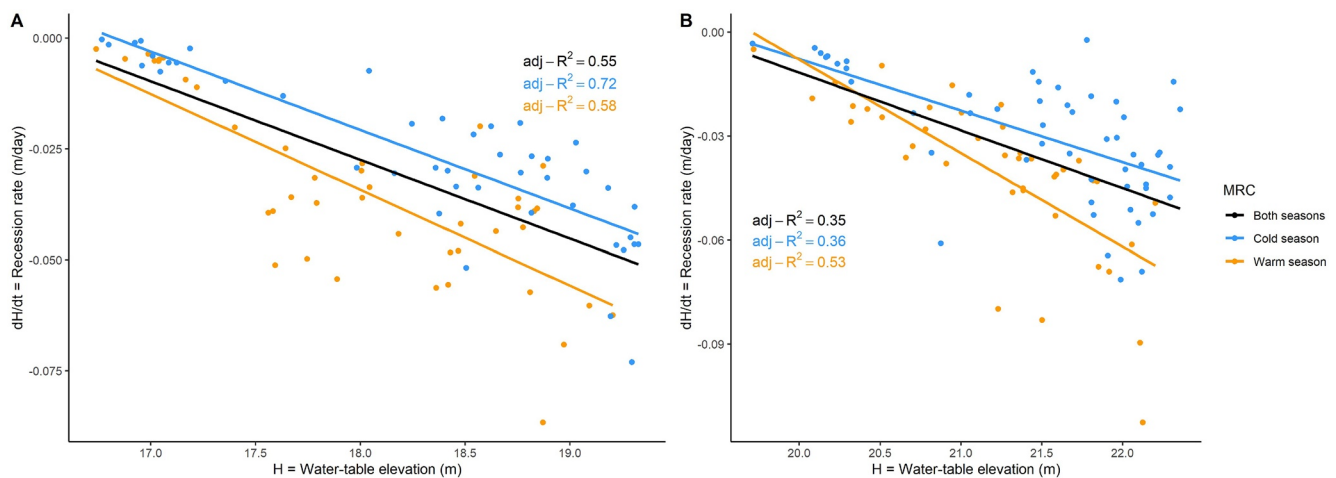


Figure 4. (a) Master Recession Curves (MRCs) for site JO-035. (b) MRCs for site BE-080. Blue points represent the observed groundwater recession data within the cold season, with the blue line indicating the cold season MRC. Orange points correspond to the observed groundwater recession data inside the warm season and the orange line represents the respective warm season MRC. Black line indicates the fitted regression line for both seasons altogether.

4. Results

4.1. Seasonality of Recession Time Constants

The black line in Figure 4a illustrates a single MRC for site JO-035, derived from a total number of 90 recession segments that were identified within the 14-year period subject to a specific parameterization of the *MRCfit.v5.1* program (see Text S1 in Supporting Information S1). The decent linear fit (adjusted R^2 of 0.55) supports the validity of the assumption that groundwater recession at the site follows a linear reservoir relation, with higher water-table elevations generally displaying faster recession rates. Figure 4a also shows both the cold season and the warm season MRC for the same site, revealing improved goodness-of-fit (adjusted R^2 of 0.72 and 0.58 respectively). For the cold season MRC, 44 recessions were detected in total, while 43 recessions were identified within the warm season. Recession segments that fell between both seasons that is, either started in late March and ended in early April or commenced in late September and stopped in early October, were not counted toward either season. The lower absolute slope of the cold season line, in comparison to the warm season, indicates that the average groundwater recession in winter occurred more slowly than in summer; indeed, the observed warm season τ_m was found to be ~ 46.3 days, whereas the recession time constant of the cold season was ~ 56.5 days. To further explore the disparity between τ_m of the seasons, we investigated the statistical significance of the relative difference between the recession rates of each season. Specifically, we utilized the Mann-Whitney U test (Mann & Whitney, 1947) to compare the two distributions of recession rates as shown in Figure 5a. At the 95% confidence level ($\alpha = 0.05$), we found that the recession rates of the warm season originated from a higher-magnitude stochastic distribution with the absolute median value of recession rates being higher in summer months. Indicative of the distinct differences between the two distributions, is also the fact that the 25th percentile of the cold season (~ -0.038 m/day) equaled approximately the median recession rate of the warm season (~ -0.037 m/day).

Accounting for seasonality at site BE-080 also resulted in a better MRC fit in comparison to the fit obtained using a single MRC fit to data from all recession events (Figure 4b). Inside the 9-year period analyzed for this site, 96 recession segments were detected in total, with 52 of them belonging to the cold season and 40 recessions occurring during the warm season. Similar to site JO-035, recessions that extended across both seasons were neglected. The hypothesis that the water-table recesses exponentially was less strong at site BE-080 (see adjusted R^2 values in Figure 4b). Nevertheless, differences between seasonal recession time constants appeared more apparent at this site (see slopes of lines in Figure 4b), with the measured warm season τ_m being ~ 37.1 days in contrast to the ~ 67.2 days for cold season. The Mann-Whitney U test confirmed that the stochastic distribution of warm season recession rates is greater in absolute terms than the respective cold season distribution (Figure 5b), with 95% confidence.

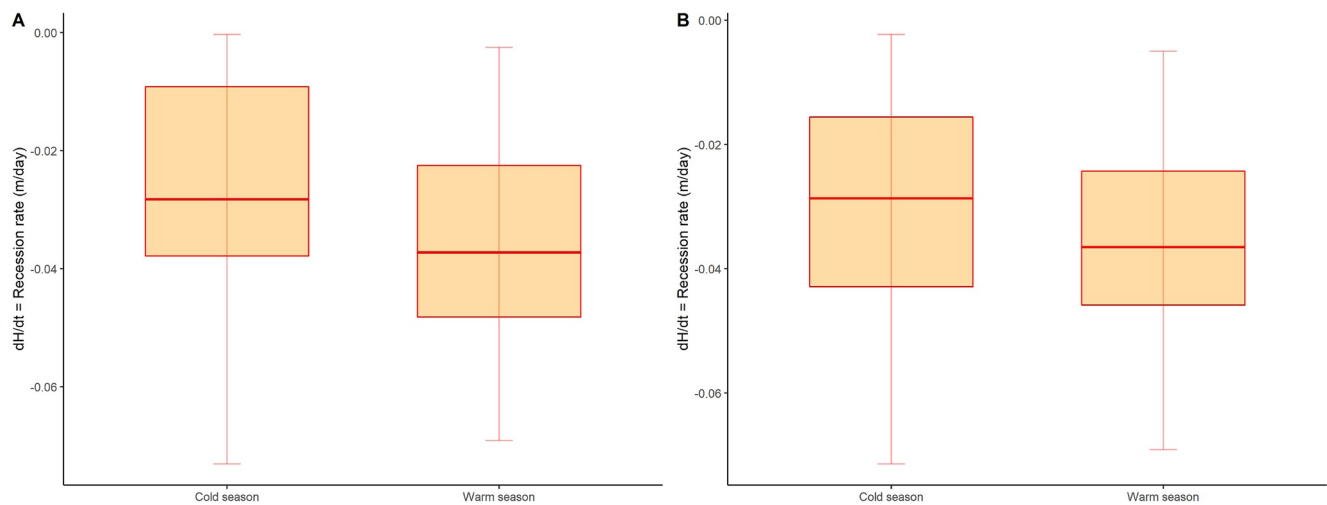


Figure 5. (a) Distributions of seasonal groundwater recession rates for site JO-035. (b) Distributions of seasonal groundwater recession rates for site BE-080.

4.2. Discrepancy in Seasonal Estimates of Groundwater Recharge Based on a Single MRC Versus Seasonal MRCs

At site JO-035, cold season groundwater recharge estimated with a single MRC, that is, using data from all identified recession events, ranged from 64 to 151 cm during the 14-year analysis period, while the cold season MRC resulted in lower estimates that ranged between 51 and 137 cm (Figure 6a). Recharge during the warm months ranged from 31 to 145 cm when using a single MRC instead of the seasonal one which increased recharge estimates to range between 41 and 159 cm (Figure 6b). At site BE-080 as well (Figures 6c and 6d), the single MRC predicted higher (lower) recharge during the cold (warm) months, with values ranging from 28 to 53 cm (15 and 49 cm) instead of 24–48 cm (17 and 57 cm) that is obtained when using the cold (warm) season MRC. The average recharge discrepancy for warm and cold seasons for JO-035 (BE-080) were 17.5% (16.0%) and -15.0% (-12.5%), respectively, when using the seasonal MRCs. It is obvious that the typical single MRC approach overestimated groundwater recharge during winter but underestimated the amount for both sites during summer. This is because averaging of the recession behavior when using data of all seasons caused the extrapolated curve to be lower than the actual points the water-table would have recessed to in the cold season (Figure S3 in Supporting Information S1), leading to increased recharge estimates. Vice-versa for summer; the real recession curve lays below the generic MRC and thus recharge was underestimated (Figure S4 in Supporting Information S1).

4.3. Estimating Intra-Annual Recession Time Constants

The models outlined in Subsections 3.3 and 3.4 can be used to obtain recession time constants for a given period within a year. To obtain estimates using the conceptual model, we first computed the two unknown parameters, viz. τ , that is, the theoretical recession time constant that discounts any influence of groundwater evapotranspiration, and d_a , the root extinction depth. To this end, median ET rates during recession periods of both seasons were obtained. For site JO-035, these were found to be 0.0057 m/day for the warm season (q_{ETW}) and 0.0031 m/day for the cold season (q_{ETC}) respectively. Corresponding ET rates for BE-080 site were 0.0058 m/day and 0.0026 m/day respectively. The specific yield for JO-035 was set to 0.15, an average value of the two soil core samples collected from the site in a previous study (Coes et al., 2007). Given the seasonal warm and cold season τ_m of 46.3 and 56.5 days respectively (see Subsection 4.1), Equations 9 and 10 yielded a τ of 76.6 days and d_a equal to 4.45 m. Using specific yield values of 0.05 (Coes et al., 2007) for BE-080, and the seasonal warm and cold τ_m of 37.1 and 67.2 days respectively, Equations 10 and 11 yielded a τ and d_a of 197.8 days and 5.3 m respectively. Along similar lines, to obtain the intra-annual recession time constants using the MLR method, we first obtained the regression parameters of Equation 11 for both the sites. For site JO-035, the derived regression parameters were $b = 66.19$, $w_1 = 0.66$, $w_2 = -6.21$, while corresponding parameters for BE-080 were 184.99, -4.86 , and -7.21 , respectively. As expected, w_2 at both the sites was negative indicating an inverse relation between τ_m and ET. For

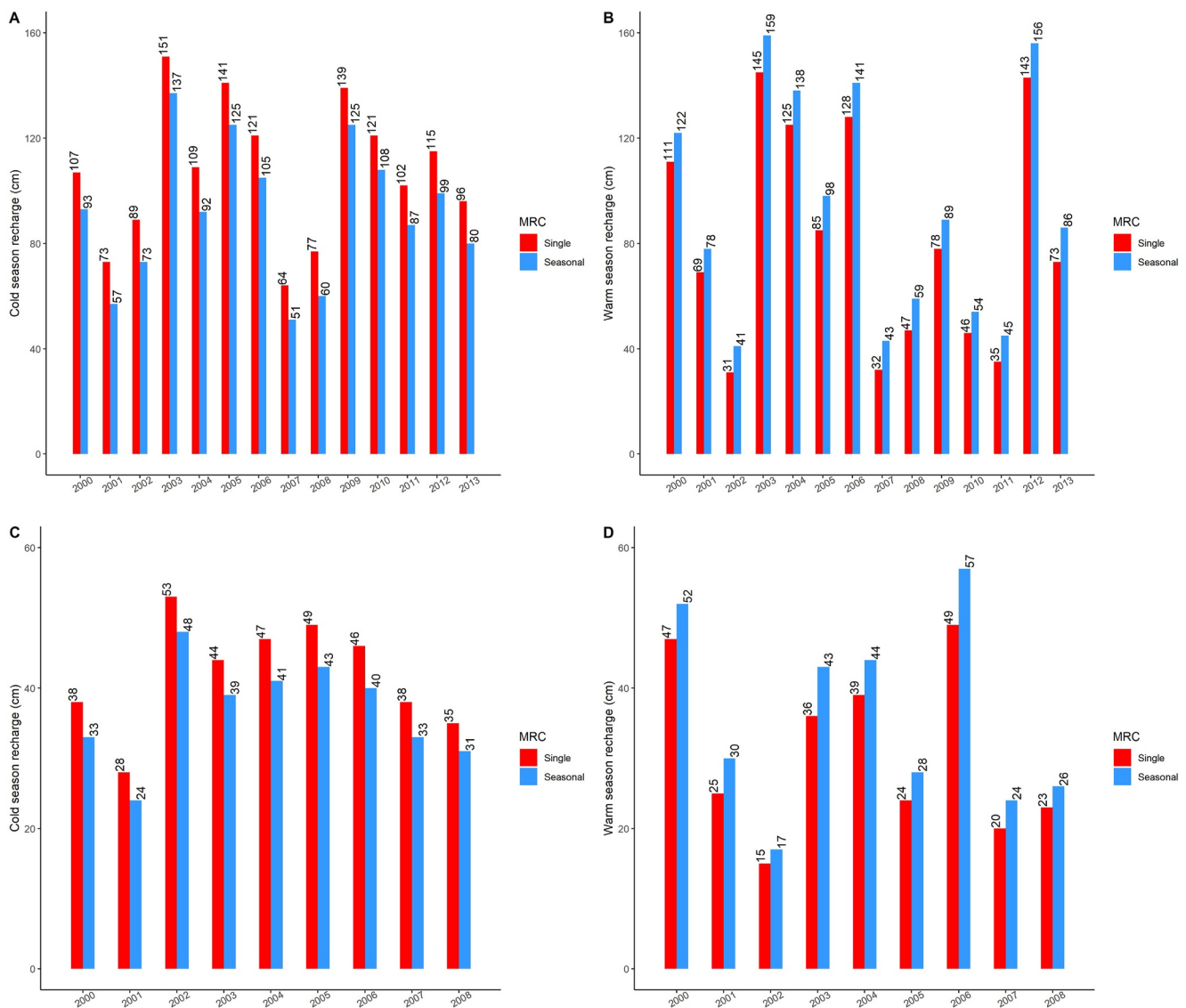


Figure 6. Cold season (a) and warm season (b) groundwater recharge estimates at site JO-035. Cold season (c) and warm season (d) groundwater recharge estimates at site BE-080. Red bars indicate recharge estimates obtained from a single Master Recession Curve (MRC), while blue bars are recharge estimates derived by the respective seasonal MRC.

both sites, the regression parameter w_1 was found to be statistically insignificant (p -value > 0.05), implying that ET is the dominant control on groundwater recession.

Next, we assessed the potential of the two models to obtain the seasonal recession time constants for alternative intra-annual periods (Table 1 and Table S1 in Supporting Information S1). The two models show promise for estimating the value of seasonal recession constants. Notably, the discrepancy in modeled τ_m as obtained based on the two methods is oftentimes much smaller than if a single MRC-based τ_m is used (see Table S1 in Supporting Information S1). It is worth highlighting that derivation of seasonal MRC or within-year MRC is not feasible for settings with a limited length of groundwater time series or a scant number of recharge events or with only a few no-recharge recession events as identified by *MRCfit.v5.1*. For these settings, the only option is to use a single MRC-based τ_m . Our results indicate that estimates of τ_m from the two models proposed here will serve as a more accurate alternative. The aforementioned models can be used for assessing seasonal recession constants in any given year and also its interannual variations. Figure S5 in Supporting Information S1 shows the seasonal (cold/warm) estimates of τ_m from both models for distinct years. Despite markedly different approaches for estimating

Table 1
Recession Time Constant (τ_m) for Different 3-Month Periods as Computed Using Single Master Recession Curve (MRC), Seasonal MRC, and Estimated Using the Proposed Models at Sites JO-035 and BE-080

Period	Observed τ_m (Single MRC)	Observed τ_m (Seasonal MRC)	MRC adj-R ² (Seasonal MRC)	Estimated τ_m (Conceptual model)	Estimated τ_m (MLR model)
Site JO-035					
December–February	55.60	63.72	0.85	61.58	65.54
March–May	55.60	176.46	0.01	48.97	47.95
June–August	55.60	28.94	0.82	44.46	38.66
September–November	55.60	46.82	0.71	53.32	54.6
Site BE-080					
December–February	57.20	69.26	0.35	76.33	63.25
March–May	57.20	31.04	0.33	49.45	49.89
June–August	57.20	28.15	0.53	33.21	34.31
September–November	57.20	41.19	0.62	62.6	63.02

τ_m , both methods show similar inter-annual variation in τ_m . Given that no such estimate can be made using the MRC method due to a lack of sufficient number of identified recession events in a cold/warm season of a given year, these estimates remain unverified.

5. Methodological Limitations and Discussions

Our mean annual recharge estimates using a single MRC were 189 and 73 cm at JO-035 and BE-080 respectively. Both estimates are comparable to the historical mean annual estimates (120 cm and 64 cm) at the same sites from Coes et al. (2007), with discrepancies originating from a difference in time period being considered in the two studies, as well as a different implementation of the WTF method. It is to be noted that should the lower end of the specific yield value be used that is, 0.11, instead of the mean value of 0.15, our mean annual recharge estimate at JO-035 using the single MRC is 139 cm. The calculated annual recharge-to-precipitation ratios (RPR) ranged from 0.86 to 1.63 at JO-035 (a gentle valley-slope site) and from 0.49 to 0.82 at BE-080 (an upland-flat site). Generally, these ratios at annual scale should be lower than one. Uncertainty in specific yield estimates though, can introduce great errors to aquifer budget terms (Liu et al., 2022). For both sites, groundwater recharge was likely overestimated because specific yield values estimated at sites where the water-table is very close to the land surface are typically higher than the actual field specific yields (Childs, 1960). Better estimates of specific yield can possibly address the above issue (Crosbie et al., 2019). Also, since groundwater monitoring wells are not necessarily always installed in groundwater discharge zones, and may receive excess water (i.e., more input from upland areas than discharge to the downslope regions) from upland areas via lateral flow, this could contribute to overestimation of recharge. As site specific observational data of ET and recharge is lacking, quantifying the sources of uncertainties in recharge estimates derived from the WTF method remains a challenge.

The models introduced here for estimating seasonal recession time constants in shallow aquifers have certain limitations. Specifically, our conceptual model relies on several assumptions, as described in Subsection 3.3, that are only approximately valid under special circumstances, at best. Notably, we assumed that the plant roots at both sites are deep enough so that d_a extends all the way below the water-table, implying that the plant species are phreatophytes that is, are directly using groundwater (Meinzer, 1923). However, absence of root sampling data from excavations at the sites precludes definitive proof. In addition, in our conceptual model, we postulated that the roots are uniformly effective over the full extent between 0 to d_a , suggesting that the partitioning of ET to vadose zone ET and groundwater ET is only dependent upon the depth to water-table (see Equation 5). This type of partitioning constitutes the simplest form of ET breakdown and it is best known as the *bucket model* approach (Hao et al., 2005; Smithwick et al., 2014). In reality, characterizing partitioning is a very challenging task controlled by variables like soil hydraulic properties and root distribution (Chen et al., 2020; Shah et al., 2007). For example, thin roots with a diameter <2 mm are most often observed at the top soil layers within the vadose zone (Di et al., 2018), whereas at deeper saturated layers thicker roots are observed as a result of waterlogging potentially

causing the death of thin roots due to low oxygen levels (Naumburg et al., 2005). With finer roots being more efficient in water uptake (Pregitzer et al., 2002), the partitioning of ET to vadose zone and saturated soil can certainly deviate from the uniformity assumption. The distribution of groundwater ET itself can also be, to a certain extent, non-uniform and it is better expressed by a simple nonlinear function of depth (Luo et al., 2009) rather than the current linear function used in Equation 5. The linear function does not sufficiently account for nonlinearities originating from heterogeneities in subsurface conductivity, root density, and moisture content. Notwithstanding these shortcomings, our simplistic conceptualization of ET from groundwater still improves the estimate of seasonal recession time constants. It is expected that more sophisticated representations of groundwater ET, which will however be more data intensive, would likely improve the estimate of seasonal recession time constants, and consequently recharge estimates.

With respect to our MLR model, as with any statistical model, possible constraints originate from the sample size which itself affects the robustness of the estimated model parameters. In the present study, the relatively high number of recessions (90 and 96 respectively) and the selection of a rolling window of size one, that is, the maximum possible number of sets (k) with a sufficient number of recessions each, allowed for a robust estimate of recession time constants. We expect the results to be sensitive to a different number of recessions (n) and subsequently the number of sets (k), and the number of recessions within each set. It is to be noted that such sensitivity is likely to vary depending on the site, as the regression p-value varies with the data. Presumably, for shorter groundwater level data records and thus a smaller number of recessions, this type of approach might not be statistically feasible and yield ineffective results. Nevertheless, our computed τ_m 's show that it is possible to obtain fair estimates of recession time constants for any period when an approximate value of ET rate and water-table height is known. Model performance may improve with choice of alternate model configurations, such as with an interaction term between H and ET in Equation 11, though small sample size might prohibit such an addition. Alternative data-based approaches, such as kernel regression (Raghav & Kumar, 2021), machine learning regression (Verrelst et al., 2012) and Bayesian regression (Liu & Kumar, 2016) etc., which have shown efficacy in many hydrologic applications, may also be explored.

Uncertainty in estimates of recession constant and recharge may also be introduced through the use of remotely sensed ET data, as the model(s) used to translate sensor observations to ET may have errors. Notably, the average annual ET for the two sites using SSEBop remote sensing product, which computes the latent heat flux based on surface energy balance principles, are 162 and 149 cm, respectively (Figure S6 in Supporting Information S1), for the period under consideration. In contrast, the corresponding ET estimates using the Global Land Evapotranspiration Amsterdam Model (GLEAM) (Martens et al., 2017), a water balance-based remote sensing product, which has shown to be competitive in model intercomparison studies (Zhang et al., 2020), are 91 and 84 cm, respectively. GLEAM estimates are more in line with the observed ET in the coastal plains of North Carolina (Liu et al., 2018). Such large discrepancies in ET are expected to influence estimates of τ_m . To assess the robustness of our results to discrepancies in ET estimates, we re-computed recession time constants for the 3-month periods of Table 1 using the alternative GLEAM ET product as well. Despite the significant difference in ET estimates based on the two ET products, Table S2 in Supporting Information S1 shows that the recession time constants estimated using GLEAM are similar to those computed using SSEBop. More importantly, just like SSEBop ET, GLEAM ET also results in improved estimates of τ_m (Table S3 in Supporting Information S1) over the use of a single τ_m . Furthermore, the relative variation of τ_m across seasons is also consistent with SSEBop-based results. The result highlights that the magnitude of annual ET, as derived based on different ET products, only minimally affects seasonal estimates of τ_m . This is because seasonal τ_m is largely determined by the relative variation in ET across seasons. All in all, the conclusion regarding the influence of ET on groundwater recession is fairly robust to the choice of ET product, as long as the ET product exhibits appropriate seasonal variations. Another source of uncertainty is the absence of data related to partitioning of ET into E and T. In our analysis, for simplicity, we also implicitly assumed that either ET retrieved from the remotely sensed data is largely contributed by transpiration (Subsection 3.3), which is the water extracted from *bls* by the plants (see Equations 6 and 7), or the transpired water is closely correlated with total ET (see Equation 11). In reality, this may not be true, depending on the contributions from soil evaporation and interception (Raghav et al., 2022). Again, an advanced partitioning of ET into E and T than the one adopted here, which could generate a more accurate estimate of the two components and their seasonal variability, is expected to further improve seasonal recharge estimates. Finally, errors may also be introduced due to the scale-mismatch between the pixel-scale ET that is used for estimating recession constant at the well location.

Despite aforementioned limitations, the results of Subsection 4.1 suggest that groundwater recessions during cold season typically occurred at lower rates than those of warm season. While it is generally expected that the recession rates are lower for lower water-table (Figures 4a and 4b), it is to be noted that recession rates in warm season are found to be higher in absolute value despite water-table being on an average lower (average water-table depth in warm months = 1.95 and 1.36 m at the two sites respectively) than cold months (average water-table depth = 1.63 and 1.01 m at the two sites respectively). This suggests that rather than any seasonal variations in precipitation, groundwater ET, which varies significantly between summer and winter, biases groundwater recession curves in summer. Seasonal groundwater recession analysis at five other sites (spanning additional three US states of Alabama, Georgia, and Virginia), where the water-table has been historically shallow as well, suggest that groundwater recession (recession constant) is faster (smaller) in warm months (Table S4 in Supporting Information S1). Notably, at three of these five sites, groundwater table depth in warm season is deeper than in cold season, but still the recession constant is smaller. This further confirms the role of groundwater ET in biasing groundwater recession constant in shallow groundwater systems. At a few other sites from North Carolina and Virginia, where the groundwater table is deeper, that is, where the contribution of groundwater ET is expected to be much smaller, the groundwater recession constant follows the seasonal variations that is reflective of the groundwater table depth, with smaller recession constants during seasons with shallower groundwater table (Table S5 in Supporting Information S1), as is expected based on Equations 1 and 2. However, absence of specific yield information for these other sites prevents seasonal recharge estimation, as well as the application of our conceptual and statistical models Subsections (3.3 and 3.4).

6. Conclusions

We examined the role of seasonal variations in groundwater ET on groundwater recession at two surficial aquifers in the NC Coastal Plain region. Our results show that higher groundwater ET rates observed in summer biased the groundwater recession curves, causing the water-table to decline faster in warmer months. Notably, the seasonal variations in the recession rate in several shallow groundwater systems cannot be explained just based on the variations in groundwater table depths. Instead, the expressed seasonality points to the contribution of groundwater ET on recession. In contrast, the seasonality of recession rates in systems with relatively deeper groundwater table is entirely explainable just based on the variations of groundwater depths. Future studies are needed to verify the universality of these findings by performing these analyses over a wider range of sites.

Estimates of seasonal recharge rates computed using seasonal MRCs show the importance of grouping recession patterns into seasonal MRC segments, in contrast to a single MRC segment that has been widely employed in previous recharge studies. Notably, differences in seasonal recharge estimates were as large as 28% depending on year and site, with overestimations occurring in the cold season and underestimations during the warm season. These findings become increasingly valuable when seasonal groundwater recharge is of great importance (Liu et al., 2021; Mollema & Antonellini, 2013; Zhang et al., 2019). The results also show that given groundwater recession rates change over seasons; therefore, it may be more appropriate to call them recession time coefficients.

The study also introduced two parsimonious novel modeling approaches to estimate recession time constants for different seasons, which can help compute seasonally varying recharge rates. The proposed methods, while being simple and data parsimonious, can still capture variations in seasonal recession constants, and are superior to the single MRC model. The proposed models are flexible and can be used to estimate recession constants for any given period during a given year (say, March–May of 2004), which is not possible using the methods currently available in the published literature. We also underscored that improved estimate of ET from groundwater, either through a more accurate but likely complex model representation and/or through use of accurate ET data products and its partitions, would likely improve the quantification of seasonal recession time constants and consequently groundwater recharge. The accuracy of the recharge estimates, however, should be further verified using data from alternative field-scale measurement tools, such as lysimeters (von Freyberg, Moeck and Schirmer, 2015) or geochemical tracers (Moeck et al., 2017), to improve these models.

Data Availability Statement

The precipitation data are available through the NOAA Climate Data Online Program: <http://www.ncdc.noaa.gov/cdo-web/>, while the groundwater data via the USGS Water Information System: <http://nwis.waterdata.usgs.gov/nwis/gw>. The SSEBop evapotranspiration data are available through the USGS Early Warning and Environmental Monitoring Program: <https://earlywarning.usgs.gov/ssebop/modis>, while the Global Land Evaporation Amsterdam Model (GLEAM) data can be obtained from <https://www.gleam.eu/>.

Acknowledgments

This work is partially supported by NSF OIA-2019561, NSF EAR-1920425, and NSF EAR-1856054.

References

- Aeschbach-Hertig, W., & Gleeson, T. (2012). Regional strategies for the accelerating global problem of groundwater depletion. *Nature Geoscience*, 5, 853–861.
- Allocca, V., De Vita, P., Manna, F., & Nimmo, J. (2015). Groundwater recharge assessment at local and episodic scale in a soil mantled perched karst aquifer in southern Italy. *Journal of Hydrology*, 529, 843–853. <https://doi.org/10.1016/j.jhydrol.2015.08.032>
- Bhaskar, A. S., Hogan, D. M., Nimmo, J. R., & Perkins, K. S. (2018). Groundwater recharge amidst focused stormwater infiltration. *Hydrological Processes*, 32, 2058–2068.
- Chen, X., Kumar, M., de B Richter, D., & Mau, Y. (2020). Impact of gully incision on hillslope hydrology. *Hydrological Processes*, 34(19), 3848–3866.
- Childs, E. C. (1960). The nonsteady state of the water table in drained land. *Journal of Geophysical Research*, 65(2), 780–782.
- Coes, A. L., Spruill, T. B., & Thomasson, M. J. (2007). Multiple-method estimation of recharge rates at diverse locations in the North Carolina Coastal Plain, USA. *Hydrogeology Journal*, 15(4), 773–788.
- Crosbie, R. S., Doble, R. C., Turnadge, C., & Taylor, A. R. (2019). Constraining the magnitude and uncertainty of specific yield for use in the water table fluctuation method of estimating recharge. *Water Resources Research*, 55(8), 7343–7361. <https://doi.org/10.1029/2019WR025285>
- Cuthbert, M. O. (2014). Straight thinking about groundwater recession. *Water Resources Research*, 50(3), 2407–2424. <https://doi.org/10.1002/2013WR014060>
- Daliakopoulos, I. N., Coulibaly, P., & Tsanis, I. K. (2005). Groundwater level forecasting using artificial neural networks. *Journal of Hydrology*, 309(1), 229–240. <https://doi.org/10.1016/j.jhydrol.2004.12.001>
- De Vries, J. J., & Simmers, I. (2002). Groundwater recharge: An overview of processes and challenges. *Hydrogeology Journal*, 10(1), 5–17.
- Delin, G. N., Healy, R. W., Lorenz, D. L., & Nimmo, J. R. (2007). Comparison of local-to regional-scale estimates of ground-water recharge in Minnesota, USA. *Journal of Hydrology*, 334(1), 231–249. <https://doi.org/10.1016/j.jhydrol.2006.10.010>
- Di, N., Liu, Y., Mead, D. J., Xie, Y., Jia, L., & Xi, B. (2018). Root-system characteristics of plantation-grown *Populus tomentosa* adapted to seasonal fluctuation in the groundwater table. *Trees*, 32, 137–149. <https://doi.org/10.1007/s00468-017-1619-2>
- Dubois, J.-M. (1995). Galperin, AM, Zaytsev, VS et Norvatov, YA, 1993. Hydrogeology and Engineering Geology. Balkema, Rotterdam, xii+367 p., 111 fig., 43 tabl., 18 × 25, 5 cm, 185\$ US. *Géographie Physique et Quaternaire*, 49(2), 322. 90-5410139-3.
- Famiglietti, J. S. (2014). The global groundwater crisis. *Nature Climate Change*, 4(11), 945–948. <https://doi.org/10.1038/nclimate2425>
- Flint, A. L., Flint, L. E., Kwicklis, E. M., Fabryka-Martin, J. T., & Bodvarsson, G. S. (2002). Estimating recharge at Yucca mountain, Nevada, USA: Comparison of methods. *Hydrogeology Journal*, 10(1), 180–204.
- Goodall, J. L., Horsburgh, J., Whiteaker, T., Maidment, D., & Zaslavsky, I. (2008). A first approach to web services for the National Water Information System. *Environmental Modelling & Software*, 23(4), 404–411. <https://doi.org/10.1016/j.envsoft.2007.01.005>
- Hao, X., Zhang, R., & Kravchenko, A. (2005). Effects of root density distribution models on root water uptake and water flow under irrigation. *Soil Science*, 170(3), 167–174. <https://doi.org/10.1097/00010694-200503000-00002>
- Healy, R. W. (2010). *Estimating groundwater recharge*. Cambridge University Press.
- Healy, R. W., & Cook, P. G. (2002). Using groundwater levels to estimate recharge. *Hydrogeology Journal*, 10(1), 91–109.
- Heppner, C. S., & Nimmo, J. R. (2005). *A computer program for predicting recharge with a master recession curve*. US Geological Survey Washington.
- Heppner, C. S., Nimmo, J. R., Folmar, G. J., Gburek, W. J., & Risser, D. W. (2007). Multiple-methods investigation of recharge at a humid-region fractured rock site, Pennsylvania, USA. *Hydrogeology Journal*, 15(5), 915–927.
- Hirsch, R. M., & De Cicco, L. A. (2015). *User guide to exploration and graphics for RivEr trends (EGRET) and dataRetrieval: R packages for hydrologic data*. US Geological Survey.
- Howe, S. S., Breton, P. L., & Chapman, M. J. (2005). *Water resources data, North Carolina, water year 2004. Volume 2: Ground-water records*. Geological Survey (US).
- Hung Vu, V., & Merkel, B. J. (2019). Estimating groundwater recharge for Hanoi, Vietnam. *Science of the Total Environment*, 651, 1047–1057. <https://doi.org/10.1016/j.scitotenv.2018.09.225>
- Kollet, S. J., & Maxwell, R. M. (2006). Integrated surface–groundwater flow modeling: A free-surface overland flow boundary condition in a parallel groundwater flow model. *Advances in Water Resources*, 29(7), 945–958.
- Kumar, M., & Duffy, C. J. (2015). Exploring the role of Domain partitioning on efficiency of parallel distributed hydrologic model simulations. *J Hydrogeol Hydrol Eng*, 12, 2. <https://doi.org/10.4172/2325-9647.1000119>
- Kumar, M., Duffy, C. J., & Salvage, K. M. (2009). A second-order accurate, finite volume–based, integrated hydrologic modeling (FIHM) framework for simulation of surface and subsurface flow. *Vadose Zone Journal*, 8(4), 873–890. <https://doi.org/10.2136/vzj2009.0014>
- Li, B., Rodell, M., Peters-Lidard, C., Erlingis, J., Kumar, S., & Mocko, D. (2021). Groundwater recharge estimated by land surface models: An evaluation in the conterminous United States. *Journal of Hydrometeorology*, 22(2), 499–522. <https://doi.org/10.1175/jhm-d-20-0130.1>
- Liu, G., Wilson, B. B., Bohling, G. C., Whittemore, D. O., & Butler, J. J. (2022). Estimation of specific yield for regional groundwater models: Pitfalls, ramifications, and a promising path forward. *Water Resources Research*, e2021WR030761. <https://doi.org/10.1029/2021WR030761>
- Liu, H., Tang, J., Zhang, X., Wang, R., Zhu, B., Li, N., et al. (2021). Seasonal variations of groundwater recharge in a small subtropical agroforestry watershed with horizontal sedimentary bedrock. *Journal of Hydrology*, 596, 125703. <https://doi.org/10.1016/j.jhydrol.2020.125703>
- Liu, X., Sun, G., Mitra, B., Noormets, A., Gavazzi, M. J., Domec, J. C., et al. (2018). Drought and thinning have limited impacts on evapotranspiration in a managed pine plantation on the southeastern United States coastal plain. *Agricultural and Forest Meteorology*, 262, 14–23. <https://doi.org/10.1016/j.agrformet.2018.06.025>

- Liu, Y., & Kumar, M. (2016). Role of meteorological controls on interannual variations in wet-period characteristics of wetlands. *Water Resources Research*, 52, 5056–5074. <https://doi.org/10.1002/2015WR018493>
- Luo, Y. F., Peng, S. Z., Khan, S., Cui, Y. L., Wang, Y., & Feng, Y. H. (2009). A comparative study of groundwater evapotranspiration functions. In *18th world imacs congress and Modsim09 international congress on modelling and simulation: Interfacing modelling and simulation with mathematical and computational sciences* (pp. 3095–3101). University Western Australia.
- Mann, H. B., & Whitney, D. R. (1947). On a test of whether one of two random variables is stochastically larger than the other. *The Annals of Mathematical Statistics*, 50–60.
- Martens, B., Miralles, D. G., Lievens, H., van der Schalie, R., de Jeu, R. A. M., Fernandez-Prieto, D., et al. (2017). GLEAM v3: Satellite-based land evaporation and root-zone soil moisture. *Geoscientific Model Development*, 10(5), 1903–1925. <https://doi.org/10.5194/gmd-10-1903-2017>
- Meinzer, O. E. (1923). *Outline of ground-water hydrology*. US Department of the Interior, Geological Survey.
- Moeck, C., Brunner, P., & Hunkeler, D. (2016). The influence of model structure on groundwater recharge rates in climate-change impact studies. *Hydrogeology Journal*, 24(5), 1171–1184.
- Moeck, C., Radny, D., Popp, A., Brennwald, M., Stoll, S., Auckenthaler, A., et al. (2017). Characterization of a managed aquifer recharge system using multiple tracers. *Science of the Total Environment*, 609, 701–714.
- Mollema, P. N., & Antonellini, M. (2013). Seasonal variation in natural recharge of coastal aquifers. *Hydrogeology Journal*, 21(4), 787–797.
- Moon, S.-K., Woo, N. C., & Lee, K. S. (2004). Statistical analysis of hydrographs and water-table fluctuation to estimate groundwater recharge. *Journal of Hydrology*, 292(1), 198–209. <https://doi.org/10.1016/j.jhydrol.2003.12.030>
- Naumburg, E., Mata-gonzalez, R., Hunter, R. G., Mclendon, T., & Martin, D. W. (2005). Phreatophytic vegetation and groundwater fluctuations: A review of current research and application of ecosystem response modeling with an emphasis on great basin vegetation. *Environmental Management*, 35(6), 726–740. <https://doi.org/10.1007/s00267-004-0194-7>
- Nimmo, J. R., Horowitz, C., & Mitchell, L. (2015). Discrete-storm water-table fluctuation method to estimate episodic recharge. *Ground Water*, 53(2), 282–292. <https://doi.org/10.1111/gwat.12177>
- Nimmo, J. R., & Perkins, K. S. (2018). Episodic master recession evaluation of groundwater and streamflow hydrographs for water-resource estimation. *Vadose Zone Journal*, 17(1), 1–25.
- Niraula, R., Meixner, T., Ajami, H., Rodell, M., Gochis, D., & Castro, C. L. (2017). Comparing potential recharge estimates from three Land Surface Models across the western US. *Journal of Hydrology*, 545, 410–423. <https://doi.org/10.1016/j.jhydrol.2016.12.028>
- Pregitzer, K. S., De Forest, J. L., Burton, A. J., Allen, M. F., Ruess, R. W., & Hendrick, R. L. (2002). Fine root architecture of nine North American trees. *Ecological Monographs*, 72(2), 293–309. [https://doi.org/10.1890/0012-9615\(2002\)072\[0293:fraonn\]2.0.co;2](https://doi.org/10.1890/0012-9615(2002)072[0293:fraonn]2.0.co;2)
- Raghav, P., & Kumar, M. (2021). Retrieving gap-free daily root zone soil moisture using surface flux equilibrium theory. *Environmental Research Letters*, 16(10), 104007.
- Raghav, P., Wagle, P., Kumar, M., Banerjee, T., & Neel, J. P. (2022). Vegetation index-based partitioning of evapotranspiration is deficient in disturbed systems. *Water Resources Research*. <https://doi.org/10.1029/2022WR032067>
- Reitz, M., & Sanford, W. E. (2020). *Modern monthly effective recharge maps for the conterminous US, 2003–2015*. US Geological Survey. <https://doi.org/10.5066/P9NRVAQ5>
- Rodell, M., Velicogna, I., & Famiglietti, J. S. (2009). Satellite-based estimates of groundwater depletion in India. *Nature*, 460(7258), 999–1002. <https://doi.org/10.1038/nature08238>
- Rorabaugh, M. I. (1960). Use of water levels in estimating aquifer constants in a finite aquifer. *International Association of Scientific Hydrology Commission of Subterranean Waters*, 52, 314–323.
- Scanlon, B. R., Healy, R. W., & Cook, P. G. (2002). Choosing appropriate techniques for quantifying groundwater recharge. *Hydrogeology Journal*, 10(1), 18–39. <https://doi.org/10.1007/s10040-001-0176-2>
- Scanlon, B. R., Jolly, I., Sophocleous, M., & Zhang, L. (2007). Global impacts of conversions from natural to agricultural ecosystems on water resources: Quantity versus quality. *Water Resources Research*, 43(3). <https://doi.org/10.1029/2006WR005486>
- Senay, G. B. (2018). Satellite psychrometric formulation of the Operational Simplified Surface Energy Balance (SSEBop) model for quantifying and mapping evapotranspiration. *Applied Engineering in Agriculture*, 34(3), 555–566. <https://doi.org/10.13031/aea.12614>
- Senay, G. B., Bohms, S., Singh, R. K., Gowda, P. H., Velpuri, N. M., Alemu, H., & Verdin, J. P. (2013). Operational evapotranspiration mapping using remote sensing and weather datasets: A new parameterization for the SSEB approach. *JAWRA Journal of the American Water Resources Association*, 49(3), 577–591.
- Shah, N., Nachabe, M., & Ross, M. (2007). Extinction depth and evapotranspiration from ground water under selected land covers. *Ground Water*, 45(3), 329–338. <https://doi.org/10.1111/j.1745-6584.2007.00302.x>
- Siebert, S., Burke, J., Faures, J. M., Frenken, K., Hoogeveen, J., Doll, P., & Portmann, F. T. (2010). Groundwater use for irrigation—a global inventory. *Hydrology and Earth System Sciences*, 14(10), 1863–1880. <https://doi.org/10.5194/hess-14-1863-2010>
- Smithwick, E. A. H., Lucash, M. S., McCormack, M. L., & Sivandran, G. (2014). Improving the representation of roots in terrestrial models. *Ecological Modelling*, 291, 193–204. <https://doi.org/10.1016/j.ecolmodel.2014.07.023>
- Sophocleous, M. A. (1991). Combining the soil water balance and water-level fluctuation methods to estimate natural groundwater recharge: Practical aspects. *Journal of Hydrology*, 124(3–4), 229–241.
- Tallaksen, L. M. (1995). A review of base flow recession analysis. *Journal of Hydrology*, 165(1–4), 349–370.
- Tashie, A. M., Mirus, B. B., & Pavelsky, T. M. (2016). Identifying long-term empirical relationships between storm characteristics and episodic groundwater recharge. *Water Resources Research*, 52(1), 21–35. <https://doi.org/10.1002/2015WR017876>
- Therrien, R., McLaren, R. G., Sudicky, E. A., & Panday, S. M. (2010). HydroGeoSphere: A three-dimensional numerical model describing fully-integrated subsurface and surface flow and solute transport. *Groundwater Simulations Group*, 35.
- Thomas, B. F., Behrangi, A., & Famiglietti, J. S. (2016). Precipitation intensity effects on groundwater recharge in the southwestern United States. *Water*, 8(3), 90. <https://doi.org/10.3390/w8030090>
- Verrelst, J., Muñoz, J., Alonso, L., Delegido, J., Rivera, J. P., Camps-Valls, G., et al. (2012). Machine learning regression algorithms for biophysical parameter retrieval: Opportunities for Sentinel-2 and-3. *Remote Sensing of Environment*, 118, 127–139.
- von Freyberg, J., Moeck, C., & Schirmer, M. (2015). Estimation of groundwater recharge and drought severity with varying model complexity. *Journal of Hydrology*, 527, 844–857.
- Wada, Y., Wisser, D., & Bierkens, M. F. P. (2014). Global modeling of withdrawal, allocation and consumptive use of surface water and groundwater resources. *Earth System Dynamics*, 5(1), 15–40. <https://doi.org/10.5194/esd-5-15-2014>
- Winner, M. D., Jr., & Coble, R. W. (1996). Hydrogeologic framework of the North Carolina coastal plain.
- Young, N. L., Lemieux, J., Delottier, H., Fortier, R., & Fortier, P. (2020). A conceptual model for anticipating the impact of landscape evolution on groundwater recharge in degrading permafrost environments *Geophysical Research Letters*. *Wiley Online Library*, 47(11), e2020GL087695. <https://doi.org/10.1029/2020gl087695>

- Zhang, B., Xia, Y., Long, B., Hobbins, M., Zhao, X., Hain, C., et al. (2020). Evaluation and comparison of multiple evapotranspiration data models over the contiguous United States: Implications for the next phase of NLDAS (NLDAS-Testbed) development. *Agricultural and Forest Meteorology*, *280*, 107810.
- Zhang, J., Wang, W., Wang, X., Yin, L., Zhu, L., Sun, F., et al. (2019). Seasonal variation in the precipitation recharge coefficient for the Ordos Plateau, Northwest China. *Hydrogeology Journal*, *27*(2), 801–813.

Influence of Shallow Groundwater Evapotranspiration on Recharge Estimation Using the Water Table Fluctuation Method

Georgios Boumis¹, Mukesh Kumar¹, John R. Nimmo², and T. Prabhakar Clement¹

¹Department of Civil, Construction, and Environmental Engineering, University of Alabama, Tuscaloosa, Alabama, USA

²Unsaturated Flow Research, Menlo Park, California, USA

Contents of this file

Text S1
Tables S1 to S5
Figures S1 to S6

Additional Supporting Information (Files uploaded separately)

NA

Introduction

The supporting information provided here consists of the parameterization of the *MRCfit.v5.1* R program for each site under study. The parameters were selected after a trial-and-error process based on subjective judgement. For a detailed description of each parameter the user is referred to Nimmo and Perkins (2018). It also includes a table (Table S1) detailing the discrepancy in estimated recession time constant (τ_m) using different methods. Table S2 is equivalent to Table 1 of the manuscript but is based on GLEAM ET estimates. Table S3 is equivalent to Table S1 of this document but uses GLEAM ET estimates. Tables S4 and S5 consist of seasonal recession time constants for additional shallow and deeper groundwater sites respectively. Figures S1 and S2 display the interrelations between precipitation, ET, and water-table depth, at both sites for a single year (2003). Sample recharge events (Figures S3 and S4) show the overestimation (underestimation) of recharge in winter (summer) when a single MRC is used. A figure (Figure S5) with seasonal (cold/warm) estimates of τ_m for multiple years, obtained via the proposed models, is also included. Figure S6 shows the annual precipitation and ET (SSEBop and GLEAM) at both sites.

Text S1.

MRCfit.v5.1 parameters for site JO-035

resplimits = c(16.724376, 19.854672)
throughorigin = FALSE
mindrytime = 2
maxdelprec = 0.5
tslength = 7
maxtick = 0.02
binsize = 0
maxslope = 0

MRCfit.v5.1 parameters for site BE-080

resplimits = c(19.58035, 22.457664)
throughorigin = FALSE
mindrytime = 1
maxdelprec = 0.5
tslength = 7
maxtick = 0.02
binsize = 0
maxslope = 0

Table S1. Discrepancy ($= 100 \times ((\tau_m \text{ from a method}) - (\tau_m \text{ from seasonal MRC})) / (\tau_m \text{ from seasonal MRC})$) in recession time constant with respect to the observed τ_m that is obtained using seasonal MRC. Calculations are only performed for sites with seasonal MRC adj-R² greater than 0.3 (see Table 1, column 4).

Period	Discrepancy in observed τ_m (Single MRC)	Discrepancy in estimated τ_m (Conceptual model)	Discrepancy in estimated τ_m (MLR model)
Site JO-035			
Dec-Feb	12.74	3.36	-2.86
Mar-May	--	--	--
Jun-Aug	-92.12	-53.63	-33.59
Sep-Nov	-18.75	-13.88	-16.61
Site BE-080			
Dec-Feb	17.41	-10.21	8.68
Mar-May	-84.28	-59.31	-60.73
Jun-Aug	-103.20	-17.98	-21.88
Sep-Nov	-38.87	-51.98	-52.3

Table S2. Recession time constant (τ_m) for different 3-month periods as computed using single MRC, seasonal MRC, and estimated using the proposed models with GLEAM ET estimates at sites JO-035 and BE-080.

Period	Observed τ_m (Single MRC)	Observed τ_m (Seasonal MRC)	MRC adj-R ² (Seasonal MRC)	Estimated τ_m (Conceptual model)	Estimated τ_m (MLR model)
Site JO-035					
Dec-Feb	55.60	63.72	0.85	60.52	60.1
Mar-May	55.60	176.46	0.01	47.67	51.84
Jun-Aug	55.60	28.94	0.82	43.9	39.46
Sep-Nov	55.60	46.82	0.71	53.1	50.14
Site BE-080					
Dec-Feb	57.20	69.26	0.35	85.62	69.59
Mar-May	57.20	31.04	0.33	46.94	33.84
Jun-Aug	57.20	28.15	0.53	34.47	31.52
Sep-Nov	57.20	41.19	0.62	59.1	93.51

Table S3. Discrepancy ($= 100 \times ((\tau_m \text{ from a method}) - (\tau_m \text{ from seasonal MRC})) / (\tau_m \text{ from seasonal MRC})$) in recession time constant with respect to the observed τ_m that is obtained using seasonal MRC. Calculations are only performed for sites with seasonal MRC adj-R² greater than 0.3 (see Table 1, column 4) using GLEAM ET estimates.

Period	Discrepancy in observed τ_m (Single MRC)	Discrepancy in estimated τ_m (Conceptual model)	Discrepancy in estimated τ_m (MLR model)
Site JO-035			
Dec-Feb	12.74	5.02	5.68
Mar-May	--	--	--
Jun-Aug	-92.12	-51.69	-36.35
Sep-Nov	-18.75	-13.41	-7.09
Site BE-080			
Dec-Feb	17.41	-23.62	-0.48
Mar-May	-84.28	-51.22	-9.03
Jun-Aug	-103.20	-22.45	-11.97
Sep-Nov	-38.87	-43.48	-127.01

Table S4. Cold (Warm) season recession time constants, τ_{mC} (τ_{mW}), for additional sites with shallow groundwater table.

USGS Site ID [State]	Data Duration	Average water- table depth	Average water-table depth (cold season)	Average water-table depth (warm season)	Observed τ_{mC}	Observed τ_{mW}	adj-R ² (Cold MRC)	adj-R ² (Warm MRC)
370712076413203 [VA]	2008-2021	2.48 m	2.42 m	2.54 m	284.22	126.14	0.10	0.39
383423077245901 [VA]	2005-2020	1.98 m	2.10 m	1.86 m	203.01	154.82	0.38	0.26
342718087285601 [AL]	2008-2021	2.59 m	2.35 m	2.83 m	53.99	31.00	0.57	0.53
322500085551201 [AL]	2009-2021	4.23 m	4.35 m	4.12 m	222.33	147.34	0.26	0.36
311009084495503 [GA]	1992-2000	3.22 m	2.79 m	3.66 m	47.32	32.47	0.49	0.62

Table S5. Cold (Warm) season recession time constants, τ_{mC} (τ_{mW}), for additional sites with deeper groundwater table.

USGS Site ID [State]	Data Duration	Average water- table depth	Average water-table depth (cold season)	Average water-table depth (warm season)	Observed τ_{mC}	Observed τ_{mW}	adj-R ² (Cold MRC)	adj-R ² (Warm MRC)
353135080524201 [NC]	2016-2021	5.22 m	5.37 m	5.08 m	538.89	216.34	0.15	0.66
371653079552101 [VA]	2005-2021	5.70 m	5.69 m	5.70 m	16.17	28.63	0.54	0.35
381002078094201 [VA]	2005-2015	8.03 m	8.21 m	7.85 m	256.78	110.07	0.20	0.65

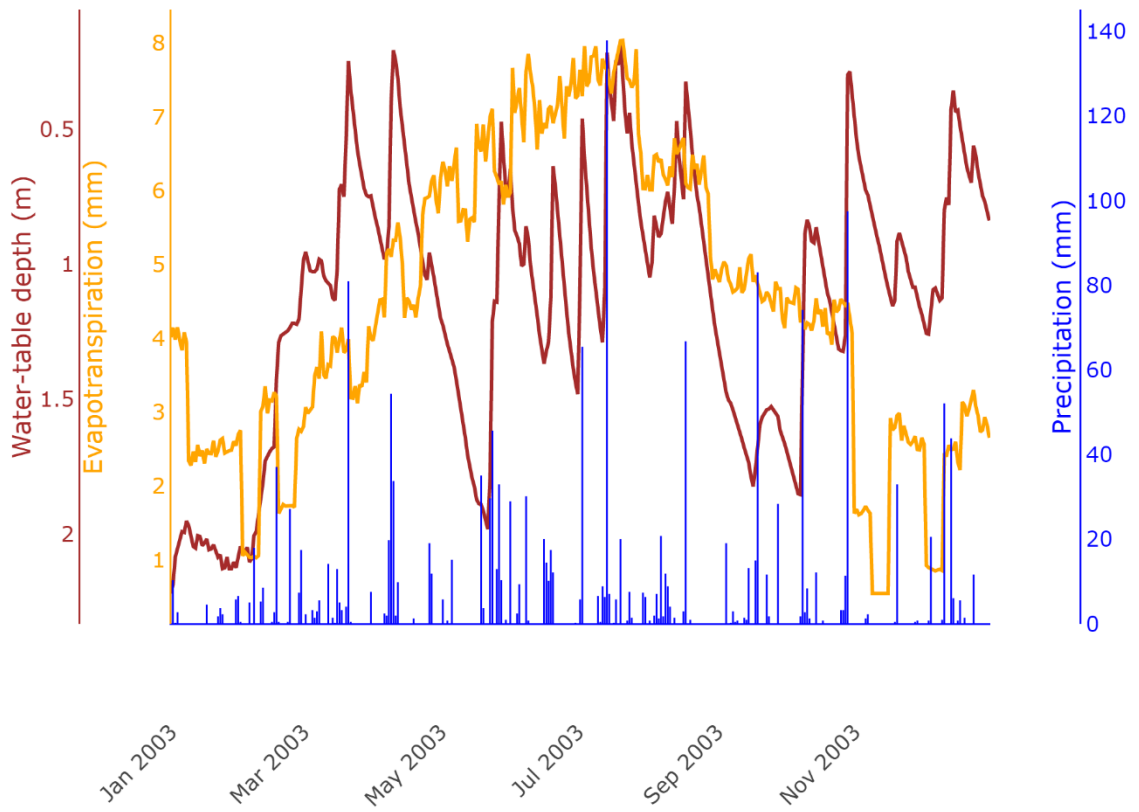


Figure S1. Precipitation (blue bars), evapotranspiration (orange line) and water-table depth (brown line) for year 2003 at site JO-035.

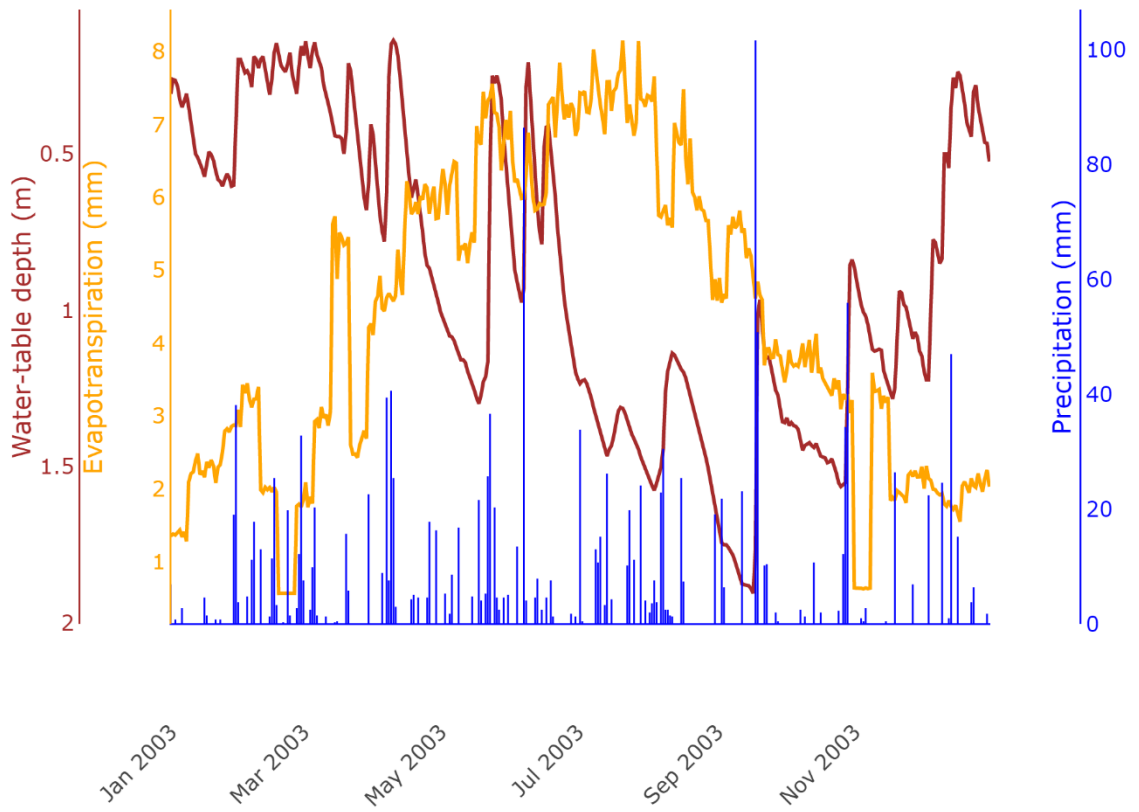


Figure S2. Precipitation (blue bars), evapotranspiration (orange line) and water-table depth (brown line) for year 2003 at site BE-080.

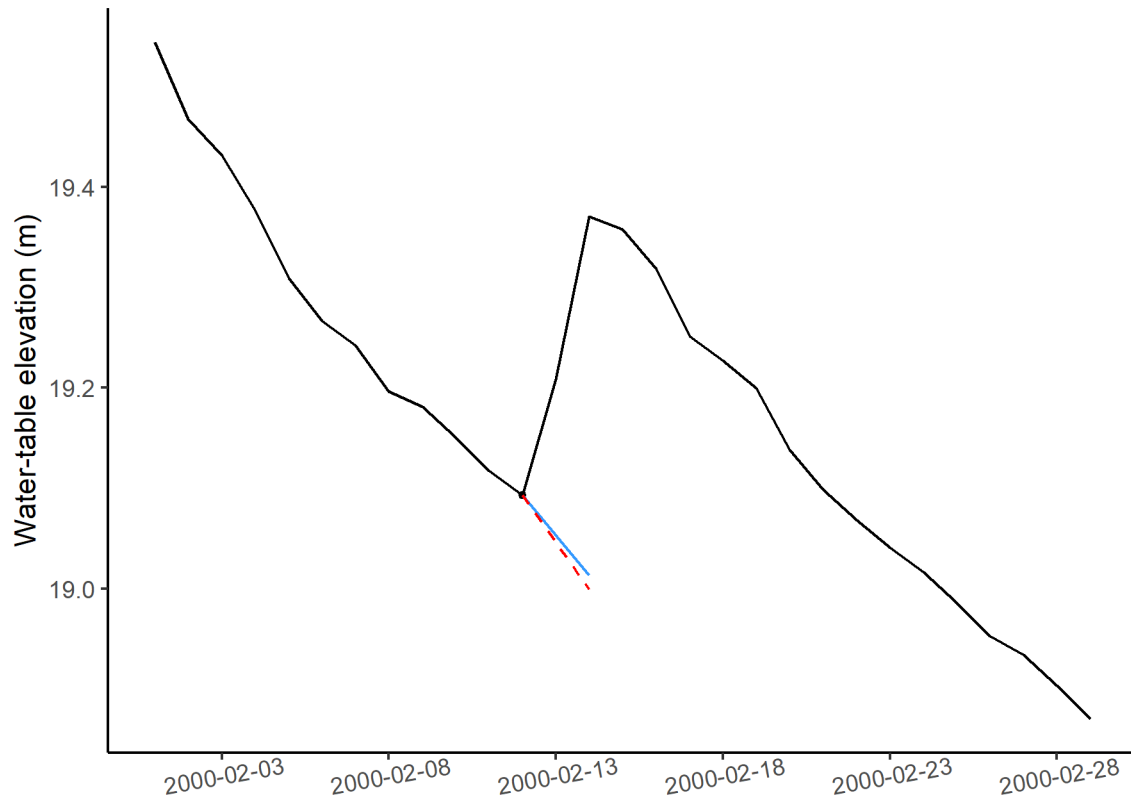


Figure S3. Example of a recharge event occurring during the cold season at site JO-035. Red dashed line indicates the extrapolated single MRC while the continuous blue line represents the extrapolated seasonal MRC.

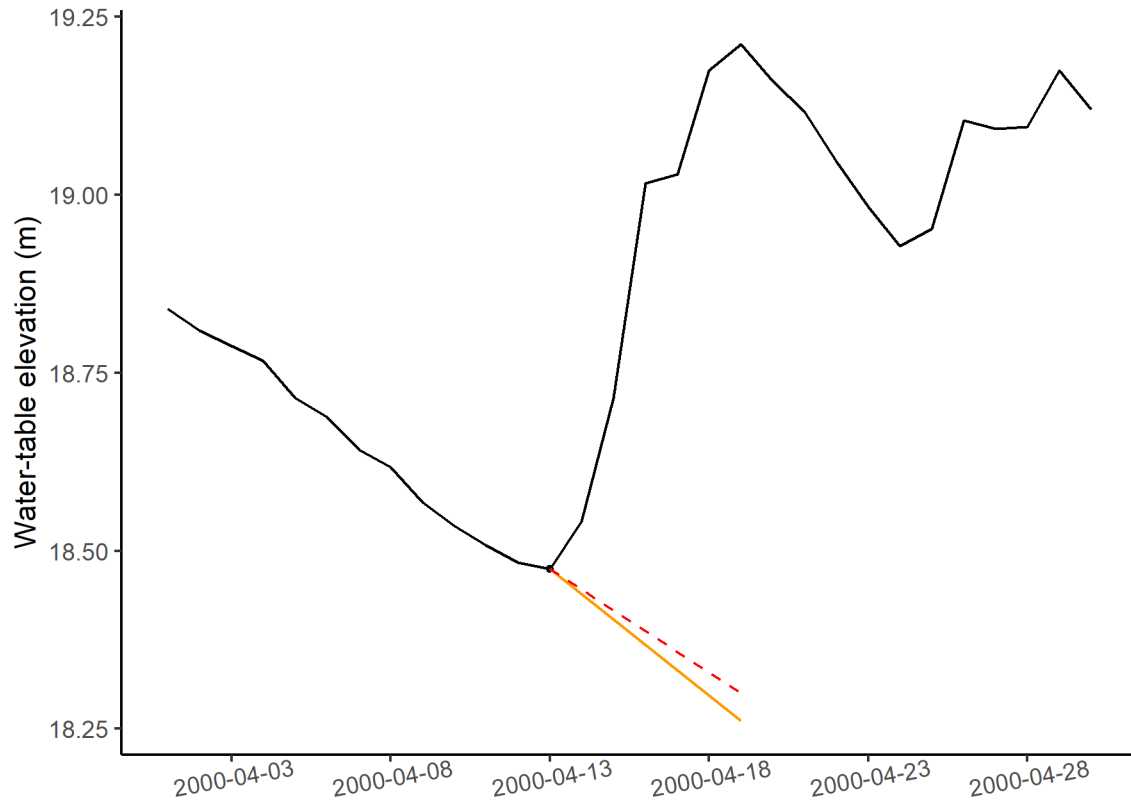


Figure S4. Example of a recharge event occurring during the warm season at site JO-035. Red dashed line indicates the extrapolated single MRC while the continuous orange line represents the extrapolated seasonal MRC.

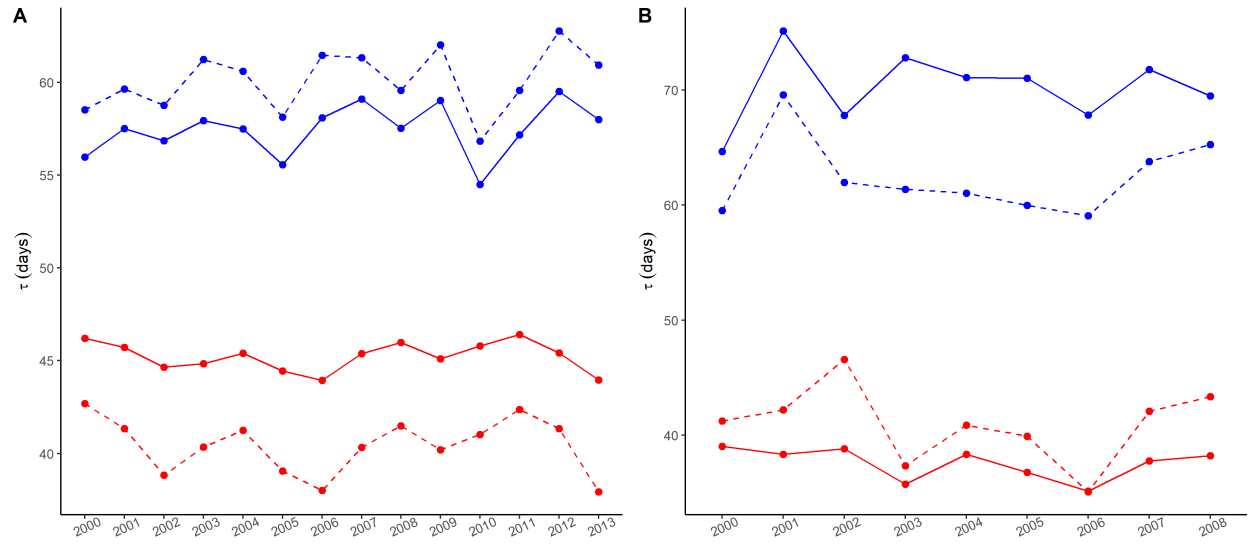


Figure S5. A) Warm season (red) and cold season (blue) τ_m as computed by the conceptual model (solid) and the MLR model (dashed) for each of the 14 years at site JO-035. **B)** Warm season (red) and cold season (blue) τ_m as computed by the conceptual model (solid) and the MLR model (dashed) for each of the 9 years at site BE-080.

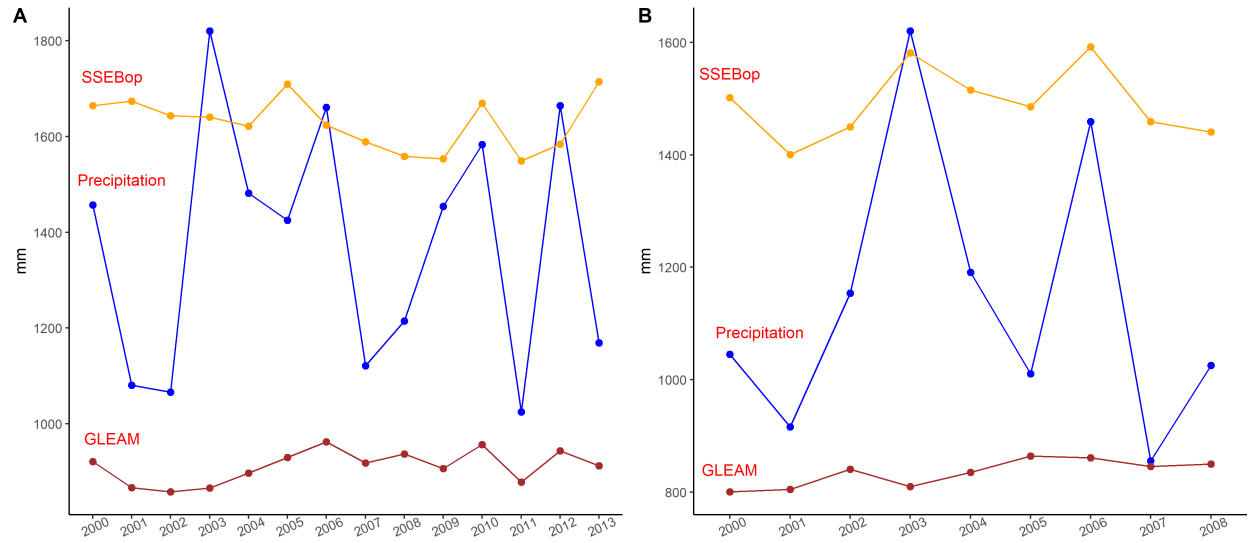


Figure S6. A) Annual precipitation (blue line), SSEBop ET (orange line) and GLEAM ET (brown line) at site JO-035. **B)** Annual precipitation (blue line), SSEBop ET (orange line) and GLEAM ET (brown line) at site BE-080.